

Article

Oxidation Behavior, Insulation Resistance, and Permeability of FeSiCr Alloys for Multilayer Inductors

Christoph Priese and Jörg Töpfer * 

Department of SciTec, Ernst-Abbe-Hochschule Jena, Carl-Zeiss-Promenade 2, 07745 Jena, Germany

* Correspondence: joerg.toepfer@eah-jena.de

Abstract: FeSiCr alloys are used as soft magnetic materials for power multilayer inductors. The alloys are typically annealed at intermediate temperatures in air during inductor fabrication to form an insulating chromium oxide layer around the alloy particles. The variation of the annealing temperature between 700 °C and 900 °C in air, and, for the first time, the variation of the oxygen partial pressure during annealing at 900 °C are studied, and their effects on the alloy's oxidation behavior, phase formation, insulation resistance, and permeability are demonstrated. The chromium oxide content increases up to about 12 wt% with annealing temperature in air, whereas it decreases to 8.2 wt% after annealing at 900 °C and 0.001% O₂. The observed mass changes during annealing confirm the various tendencies towards oxidation. This oxidation behavior is reflected in an increase in the insulation resistance with annealing temperature or in a resistance reduction with decreasing oxygen partial pressure. The permeability decreases from $\mu = 22$ after annealing at 700 °C to $\mu = 18.5$ at 900 °C in air. The reduction of p_{O_2} during annealing at 900 °C leads to an increase in permeability up to $\mu = 22.5$ at $p_{O_2} = 0.001\% O_2$. The results can be used to design cofiring strategies using reduced oxygen partial pressure for new composite multilayer inductive components consisting of FeSiCr- and ferrite layers in combination with silver metallization.



Citation: Priese, C.; Töpfer, J. Oxidation Behavior, Insulation Resistance, and Permeability of FeSiCr Alloys for Multilayer Inductors. *Alloys* **2022**, *1*, 288–297. <https://doi.org/10.3390/alloys1030019>

Academic Editor:
Konstantinos Georgarakis

Received: 21 July 2022
Accepted: 29 November 2022
Published: 13 December 2022

Publisher's Note: MDPI stays neutral with regard to jurisdictional claims in published maps and institutional affiliations.



Copyright: © 2022 by the authors. Licensee MDPI, Basel, Switzerland. This article is an open access article distributed under the terms and conditions of the Creative Commons Attribution (CC BY) license (<https://creativecommons.org/licenses/by/4.0/>).

Keywords: Fe–Si–Cr alloys; chromium oxide layer; oxidation behavior; soft magnet; permeability

1. Introduction

Soft magnetic materials and composites (SMC) have numerous applications in modern portable electronic device applications [1]. The need of miniaturization and the low profile of inductive components for portable devices has led to the development of new power inductive devices. This is in line with the observed trend from one DC–DC converter in the power circuitry to a point-of-load (POL) concept with many smaller converters as a power source for individual ICs or modules. Moreover, the operating voltages of modules in a device might be different, requiring individual and miniaturized DC–DC converters to convert the power provided by the battery into the various circuit blocks. FeSiCr alloys have been proposed as suitable magnetic materials for the fabrication of power multilayer inductors [2,3]. As compared to Ni–Cu–Zn ferrites, which are typically used in multilayer inductors, the soft magnetic alloys have benefits of high saturation magnetization and good DC-superposition characteristics and, hence, are able to withstand higher current densities without a significant reduction of the inductance [2,3]. One critical issue is the low resistivity of the alloy. Low power losses, P_v , of the soft magnetic alloy are required for high-frequency applications. Since eddy current losses P_e are a major contribution to P_v , the resistivity of the alloy needs to be increased in order to reduce P_e . Therefore, it is very important to provide sufficient insulation resistance, which is realized by creating a thin insulating oxide layer at the surface of the alloy particles during annealing and multilayer fabrication. It was demonstrated that high compaction pressures are needed to achieve sufficient densification, and that subsequent annealing in the temperature range between 700 °C and 850 °C leads to the formation of an insulating chromia layer with the

resistivity increasing with annealing temperature [4]. Many other studies have focused on increasing the resistivity by coating the alloy particles. Insulating coatings are typically classified as organic, inorganic, and composite coatings. Organic coatings are primarily thermosetting materials, such as epoxy resins, phenolic resins or polyimides. Examples of inorganic coatings include phosphates [5], silica [6], MgO [7], alumina [8], or ferrites [9].

Another problem in multilayer chip fabrication arises from the interaction of FeSiCr with the Ag inner electrode material during thermal processing in air. It was observed that Ag reacts with the Cr₂O₃ layer to form semiconducting AgCrO₂ delafossite-type oxide, reducing the insulation resistance and decreasing the inductor performance [10]. It has been observed that the annealing of FeSiCr-based multilayer inductors in nitrogen allows us to enhance the inductance by suppressing non-magnetic phase formation, but re-annealing in air is required to generate sufficient insulation resistance [11]. Thus, it seems that the oxygen partial pressure is another variable in addition to the annealing temperature to tailor the electromagnetic properties of FeSiCr alloys and the corresponding inductors. However, the effect of oxygen partial pressure upon annealing on the oxidation layer formation and the corresponding electromagnetic properties has not been systematically studied. Hence, it is desirable to investigate the role of oxygen partial pressure during annealing for the performance optimization of FeSiCr-based power multilayer inductors. In addition, a new concept of combining FeSiCr and Ni–Cu–Zn ferrites with Ag metallization to give a composite multilayer inductor was proposed recently [12], and annealing protocols include T and p_{O_2} as variables as well.

In this study, we have investigated, for the first time, the influence of oxygen partial pressure during annealing at 900 °C of a FeSiCr alloy on the phase formation, insulating Cr oxide layer formation, resistivity, and permeability. We contrast the effect of the annealing temperature in air with that of the oxygen partial pressure (from 0.21 atm down to 10^{−5} atm) during the annealing of FeSiCr compacts at 900 °C. The results indicate that annealing at 900 °C under lower p_{O_2} leads to decreasing insulation resistance and higher permeability. Annealing at intermediate p_{O_2} , on the other hand, provides sufficient insulation resistance and opens a new process window for the firing of multilayer power inductors.

2. Materials and Methods

A commercial FeSiCr powder was used with a composition of 90.3 wt% Fe, 5.4 wt% Si, and 4.3 wt% Cr (Chung Yo Materials Co., Ltd., Kaohsiung, Taiwan). The powder was mixed with a polyvinyl alcohol solution and dried at 95 °C. Pellets and toroids were uniaxially dry pressed with a pressure of 100 MPa. The samples were heated for binder burnout with 1 K/min to 300 °C and annealed for 5 h in air. In the first experimental series, the samples were further annealed with a 5 K/min heating and cooling rate to temperatures between 700 °C and 900 °C with a dwell time of 1 h. In the second series, the samples were annealed at 900 °C with a 1 h dwell time in a gas atmosphere with oxygen partial pressures between 0.21 atm (21%) and 10^{−5} atm (0.001%) using a computer-controlled gas-mixing unit with mass flow controllers. The p_{O_2} was measured directly at the sample position in the tube furnace with a zirconia-based oxygen sensor system (Zirox GmbH, Greifswald, Germany).

The specific surface area S of the powders was determined from nitrogen adsorption isotherms (BET, Nova 2000, Quantachrome Instruments, Boynton Beach, FL, USA); a mean particle size d_{BET} was estimated using as $d_{BET} = 6/\rho \cdot S$ (with density ρ ; assuming spherical particles). The particle size was characterized using laser diffraction (Mastersizer, Malvern Panalytical GmbH, Kassel, Germany). The shrinkage of a cylindrical compact was measured using a Netzsch DIL402 dilatometer (Netzsch-Gerätebau GmbH, Germany) during heating to 1000 °C with a 5 K/min heating rate. Thermal analysis was performed using a TG/DTA 92-16.18 system (Setaram, Caluire, France). The microstructure of the samples was studied on polished samples with a scanning electron microscope (SEM, Ultra 55, Zeiss Microscopy GmbH, Jena, Germany). Elemental analysis was performed using a Bruker EDX system. The phase formation of the materials was evaluated using X-ray diffraction (XRD) with Cu-K α radiation (15–90°, 3 s, 0.015°/step, Advance D8, Bruker

AXS, Karlsruhe, Germany). Rietveld refinements were performed using the software Topas version 6 (Bruker AXS). The resistivity of the samples was measured using a two-point measurement set-up after contacting the samples with silver paste. The permeability of sintered toroids was measured using an Agilent E4991A impedance/material analyzer (Keysight Techn., Santa Rosa, CA, USA) in the frequency range from 1 MHz to 1 GHz.

3. Results

The morphological properties of the FeSiCr powder were studied. The particle size distribution as obtained from laser diffraction revealed a mean particle size of $d_{50} = 10.3 \mu\text{m}$ (Figure 1a) with a broad distribution of sizes ($d_{10} = 4.1 \mu\text{m}$, $d_{90} = 28.6 \mu\text{m}$). The specific surface area was found to be $S = 0.3 \text{ m}^2/\text{g}$. This translates into a mean particle size of the primary particles of $d_{\text{BET}} = 2.6 \mu\text{m}$. SEM micrographs confirmed that the powder consisted of agglomerates with a size between 5 and 30 μm , built from smaller particles of around 1–3 μm in size.

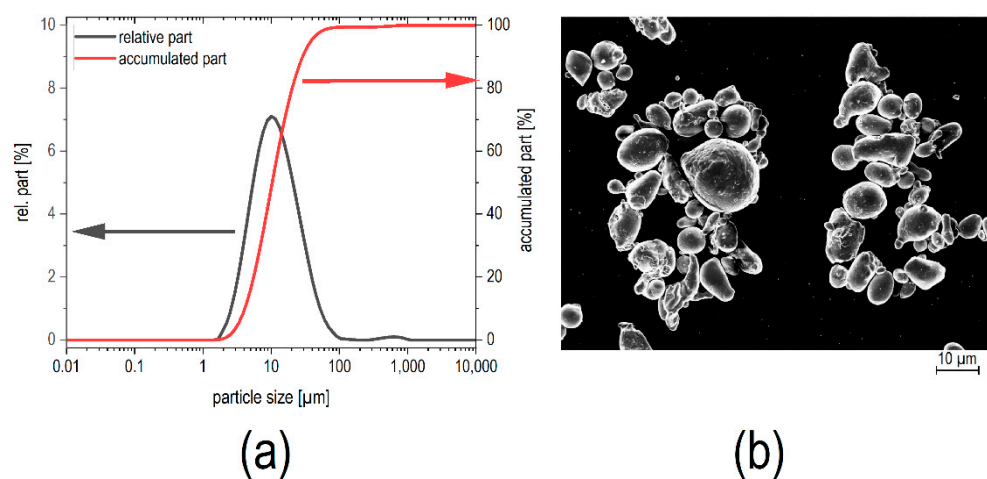


Figure 1. Particle size distribution (a) and SEM micrograph (b) of the FeSiCr powder.

The oxidation behavior of the FeSiCr powder was investigated using thermal analysis. The mass gain of the powder as a function of temperature, as determined with thermogravimetry (TG), signaled the start of an oxidation process at about 300 °C in air (Figure 2a), slowly increasing into a significant mass increase at about 600 °C, and reaching a mass gain of about 1.2% at 900 °C. Contrarily, no mass gain was observed in a gas atmosphere with $p_{\text{O}_2} = 10^{-5} \text{ atm}$. Simultaneously, the expansion of a powder pellet as a function of temperature in air atmosphere determined using a dilatometer indicated an almost constant expansion up to a maximum at about 625 °C, where the thermal expansion of the FeSiCr phase seemed to be overshadowed by another process leading to shrinkage at a higher temperature (Figure 2a). The observed mass gain originated from partial oxidation of the alloy and the formation of a layer of Cr_2O_3 (as shown later). This tendency towards oxidation was also monitored by measuring the weight change of the samples upon annealing. Annealing for 1 h in air led to a mass gain increasing with temperature (Figure 2b), reaching 2% at 900 °C. On the other hand, the observed mass gain decreased with decreasing partial pressure in the atmosphere during annealing for 1 h at 900 °C (Figure 2c), indicating a significant lower tendency towards oxidation and Cr_2O_3 formation.

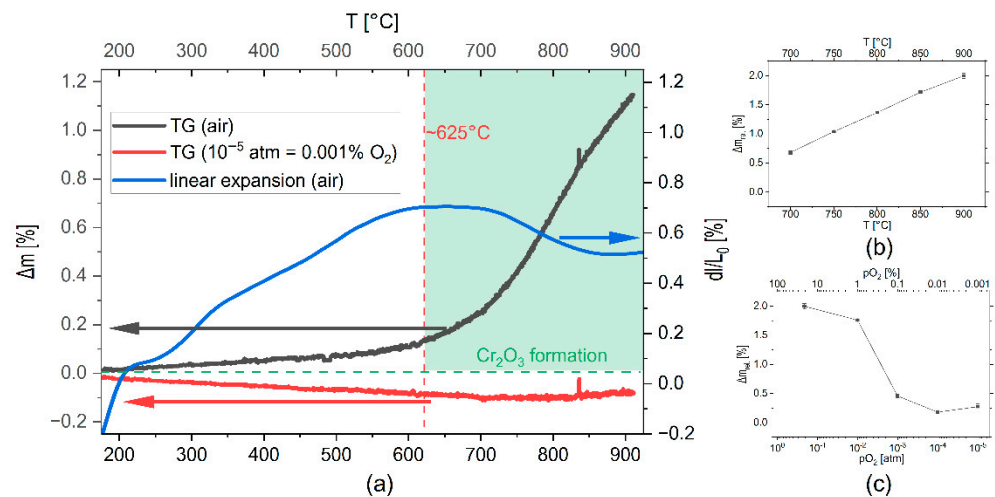


Figure 2. Thermal analysis (TG) and mass change of FeSiCr powder in air with $p_{O_2} = 0.21$ atm and gas atmosphere with $p_{O_2} = 10^{-5}$ atm and dilatometric shrinkage curve in air (a) and the mass change of pellets from FeSiCr powder during annealing for 1 h at different annealing temperatures in air (b) and at different oxygen partial pressures at 900 °C (c).

We also monitored the temperature and oxygen partial pressure during annealing in the furnace next to the sample position. The obtained in situ annealing protocols are shown in Figure 3. For annealing at various temperatures in air, the observed temperature—time protocols indicated a regular annealing process; the p_{O_2} was close to the expected value of 0.21 atm (Figure 3a). However, during annealing at various oxygen partial pressures, a different picture emerged: the p_{O_2} remained stable and constant in air atmosphere, but with nominally decreasing oxygen partial pressure, the p_{O_2} signal from the oxygen sensor decreased below the nominal p_{O_2} value already during the heating period, showing much lower values of p_{O_2} during the dwell time of the anneals. For example, at nominal $p_{O_2} = 10^{-5}$ atm, the p_{O_2} close to the sample position rapidly decreased upon heating and reached values as low as 10^{-16} atm during heating at 900 °C. This behavior demonstrated that FeSiCr soaked up all available oxygen in the gas atmosphere with reduced oxygen concentration, thus locally generating very reducing atmospheric conditions.

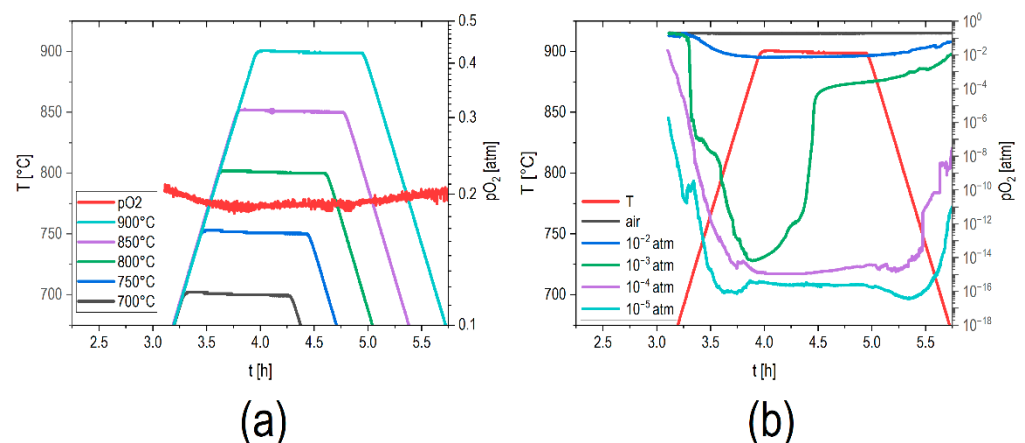


Figure 3. Annealing protocols: annealing at various temperatures in air (a), and at 900 °C (b) at different oxygen partial pressures p_{O_2} .

The samples obtained after annealing at different temperatures in air, or at different p_{O_2} values at 900 °C, were investigated using electron microscopy. EDX maps of samples annealed in air between 700 and 900 °C indicated the formation of a Cr_2O_3 layer at the surface of the alloy particles (Figure 4). The O- and Cr-maps showed a layer of Cr and O

connecting the larger alloy particles, with the thickness of the Cr_2O_3 layer increasing with annealing temperature (Figure 4). This tendency towards oxidation and the oxide layer formation agrees well with the results from thermogravimetry (TG, Figure 2a) and the mass change during annealing (Figure 2b), indicating an enhancement of mass with annealing temperature.

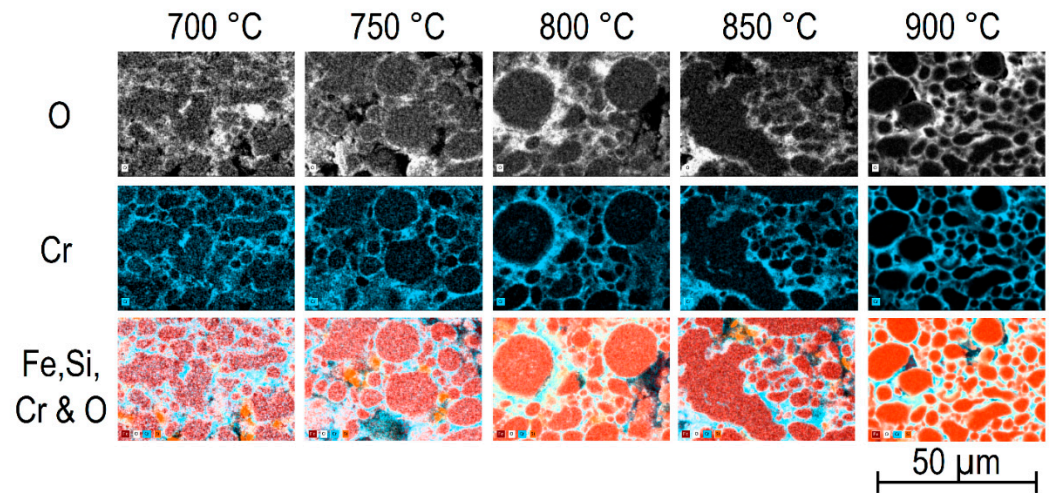


Figure 4. EDX maps of oxygen (white), chromium (blue), iron (dark red), and silicon (orange) of the FeSiCr samples annealed at various temperatures in air.

Annealing of the samples at 900 °C at different reduced oxygen partial pressures from 0.21 atm down to 10^{-5} atm was mirrored in less intense oxidation and Cr_2O_3 surface layer formation as compared to air (Figure 5). Correspondingly, the TG curve recorded during annealing in nitrogen with $p_{\text{O}_2} = 10^{-5}$ atm did not reveal any mass uptake (Figure 2a), and the mass change of the samples during a 1 h anneal at 900 °C in that gas atmosphere was very small (Figure 2c). These findings indicate that the formation of a Cr_2O_3 surface layer was less pronounced under decreasing p_{O_2} in the surrounding gas atmosphere.

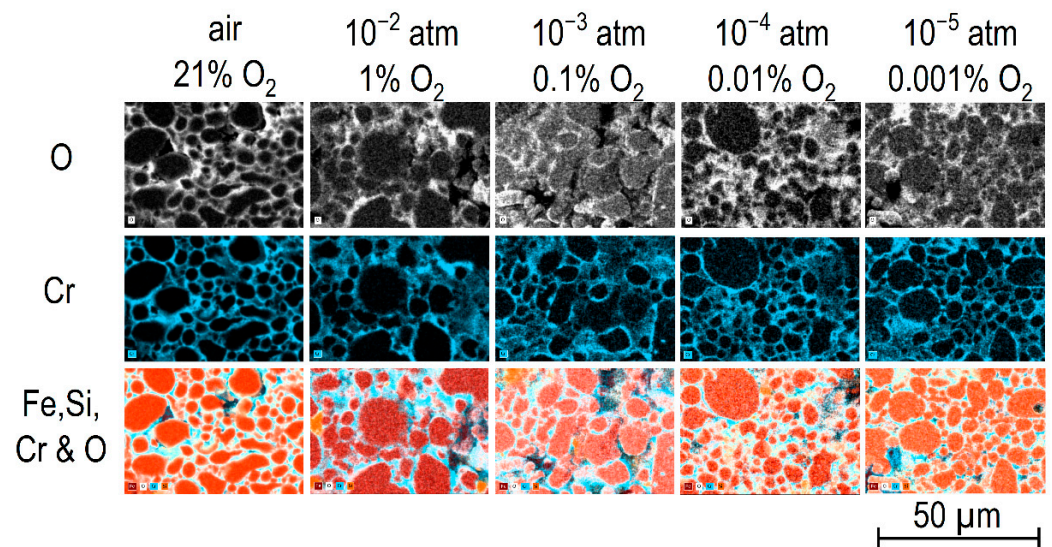


Figure 5. EDX maps of oxygen (white), chromium (blue), iron (dark red), and silicon (orange) of the FeSiCr samples annealed at various oxygen partial pressures at 900 °C.

In addition, the element concentrations of Fe, Si, and Cr in the FeSiCr particles were determined using EDX (measurement of five point-scans in the particle centers). It is

interesting to note, that after annealing in air, the Cr concentration within the alloy particles decreased with increasing annealing temperature, whereas the Fe concentration increased, and the Si content remained more or less unchanged (Figure 6a). This observation might be interpreted as the increasing diffusion of Cr out of the alloy particles with increasing annealing temperature, as the formation of the Cr_2O_3 surface layer requires the diffusion of Cr from the bulk of the particles to the surface. After annealing at 900 °C, the Cr concentration in the alloy particles decreased to about 1 wt% as compared to about 4% in the initial alloy. Consequently, the Fe concentration in the alloy particles increased. If the samples were annealed at 900 °C in reduced p_{O_2} , the Cr concentration in the alloy slightly increased with decreasing p_{O_2} , indicating the reduced formation of a chromia surface layer and, hence, increased Cr content in the alloy particles (Figure 6b).

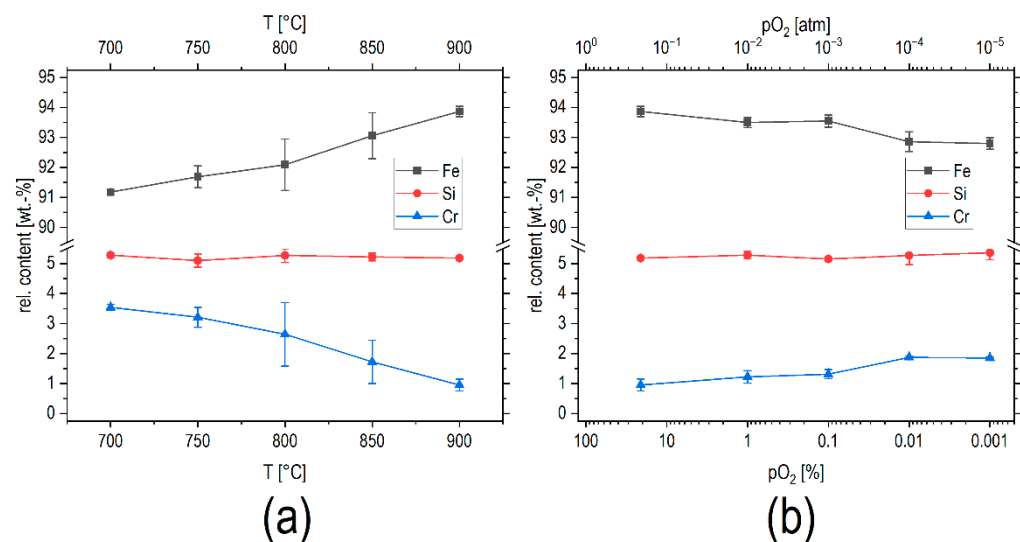


Figure 6. Element concentrations from EDX scans in FeSiCr particles in samples annealed at various temperatures in air (a) and at 900 °C under various oxygen partial pressures (b).

The results of an XRD study confirm the tendency towards oxidation upon annealing in air (Figure 7a). The initial alloy powder exhibited peaks of the alloy with a body-centered lattice typical of α -Fe [13]. Peaks of a corundum-type structured Cr_2O_3 phase [14] started to appear at 750 °C with their intensity increasing with the annealing temperature. After annealing at 900 °C, the main peaks of chromia clearly appeared. The concentration of the formed Cr_2O_3 phase was determined using Rietveld refinements, and the results are shown in Figure 8a. The chromia content was practically zero in the initial powder and increased to 12.2(3) % after annealing at 900 °C. Simultaneously, the lattice parameter a_0 of the body-centered cubic alloy phase decreased from $a_0 = 2.8601(1)$ Å of the initial alloy to $a_0 = 2.8580(1)$ Å for the 900 °C annealed sample. The decrease in the cubic lattice parameter reflects the change in the alloy composition, as Cr tended to diffuse to the alloy particle surface to be oxidized into Cr_2O_3 ; therefore, the alloy contained less Cr and more Fe with increasing annealing temperature (Figure 6a). It has been demonstrated that the cubic lattice parameter in the body-centered Fe–Cr alloy system increases with the Cr content, even more than expected according to linear Vegard’s rule [15,16].

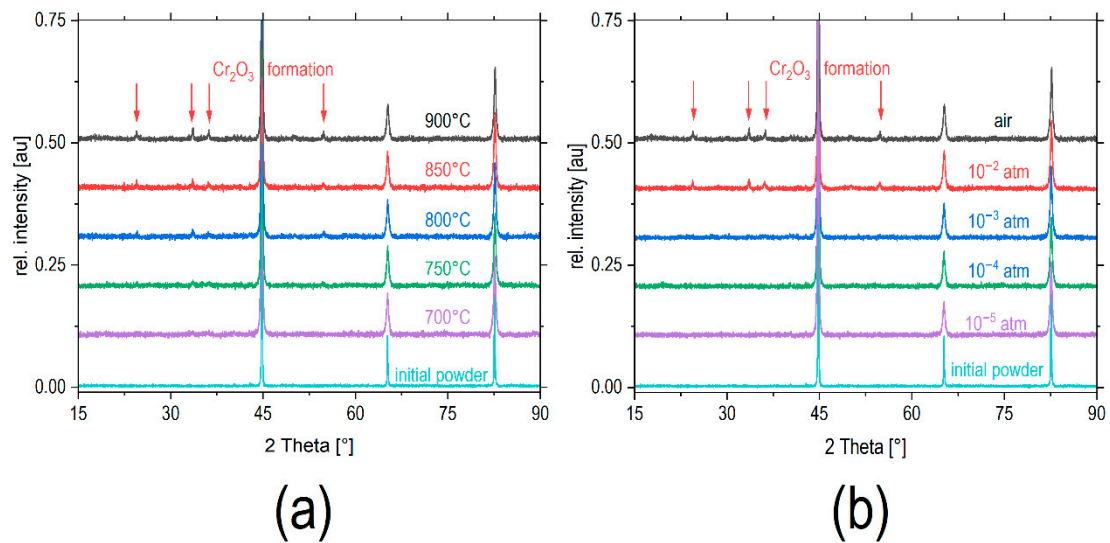


Figure 7. XRD of FeSiCr samples annealed at various temperatures in air (a) and at 900 °C under various oxygen partial pressures (b).

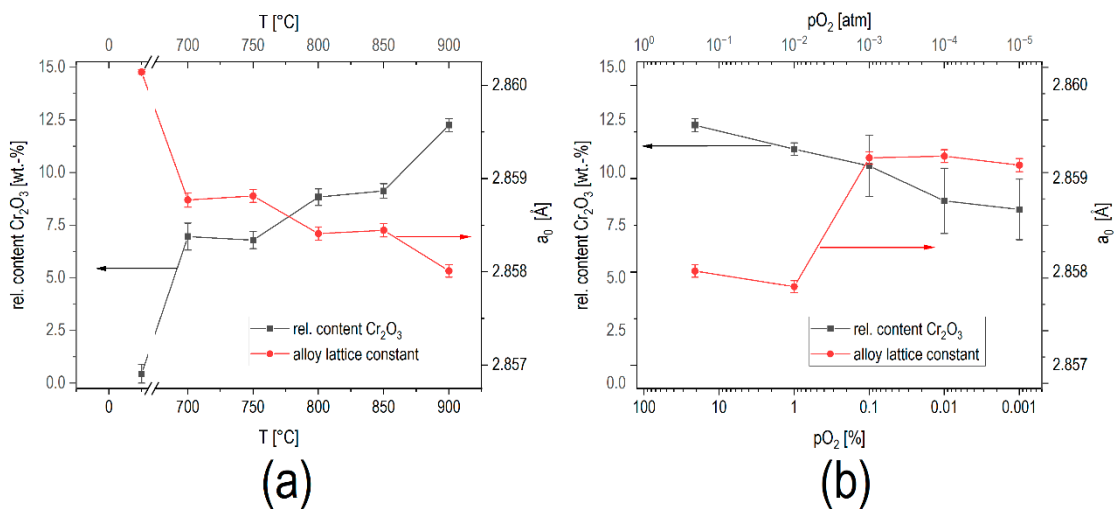


Figure 8. Cr_2O_3 concentration and alloy cubic lattice parameter a_0 of FeSiCr samples annealed at various temperatures in air (a) and at 900 °C under various oxygen partial pressures (b).

If the samples were annealed at 900 °C in various oxygen partial pressures, then the tendency towards the formation of Cr_2O_3 , as observed in air, was significantly reduced. After annealing in gas atmospheres with lower p_{O_2} , the intensity of the Cr_2O_3 peaks decreased (Figure 7b). Rietveld refinements confirmed a decrease in the Cr_2O_3 concentration in the annealed samples and reached about 8(1) wt% at $p_{\text{O}_2} = 10^{-5}$ atm (Figure 8b). At the same time, the cubic alloy lattice parameter increased with decreasing p_{O_2} , indicating an increase in the Cr content in the alloy and, consequently, less Cr_2O_3 surface layer formation (Figure 8b).

The formation of insulating Cr_2O_3 layers at the surface of the alloy particles directly affected the electrical resistivity. The increasing Cr_2O_3 layer thickness formed with increasing annealing temperature in air led to an increase in resistivity by about one order of magnitude (Figure 9a). Similar results were reported by Hsiang et al. [4]. On the other hand, a decrease in p_{O_2} at 900 °C tended to slow down the formation of this chromia surface layer (Figure 8b). Consequently, a reduction of resistivity by about one order of magnitude was observed upon changing the p_{O_2} from air to 10^{-5} atm (Figure 9b).

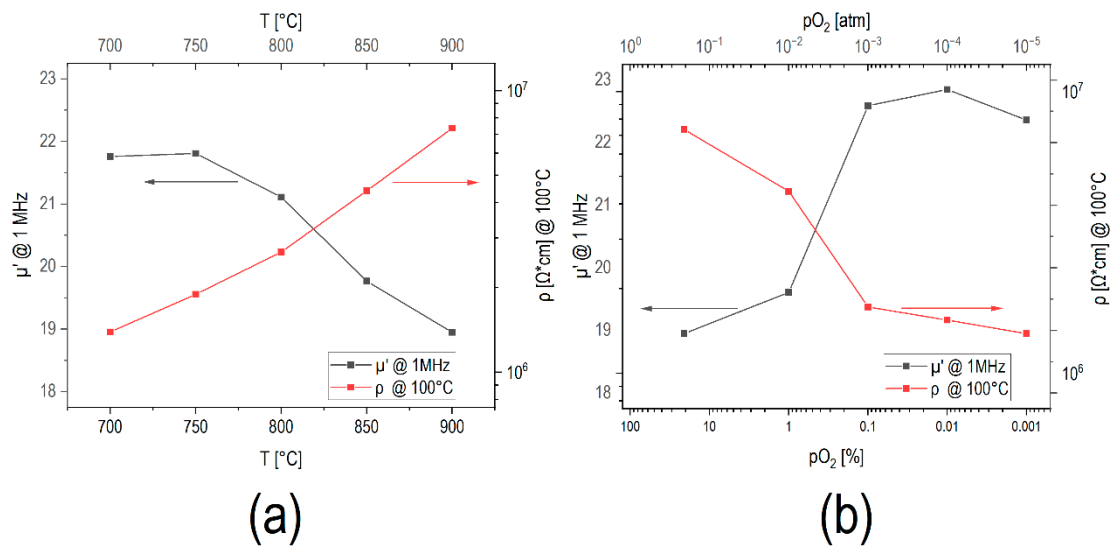


Figure 9. Permeability (at 1 MHz) and resistivity (at 100 °C) of FeSiCr samples annealed at various temperatures in air (a) and at 900 °C under various oxygen partial pressures (b).

The permeability at 1 MHz is shown as function of the annealing temperature in Figure 9, with the corresponding permeability spectra in Figure 10. Samples annealed at 700 °C exhibited a permeability of about $\mu' = 22$. It has been demonstrated that higher compaction pressure results in a larger final density of the pressed and annealed samples [4]. Compacting with 800 MPa pressure was shown to yield a permeability of $\mu' = 34$, and subsequent annealing at 750 °C was found to increase the permeability to about $\mu' = 38$ only [4]. This indicates that plastic deformation of the alloy particles seemed to be the major mechanism for the densification of the samples, whereas sintering and grain growth seemed to play a minor role only. This is consistent with the observed small shrinkage of the samples during annealing and with the almost zero shrinkage in the dilatometric curve (Figure 2a).

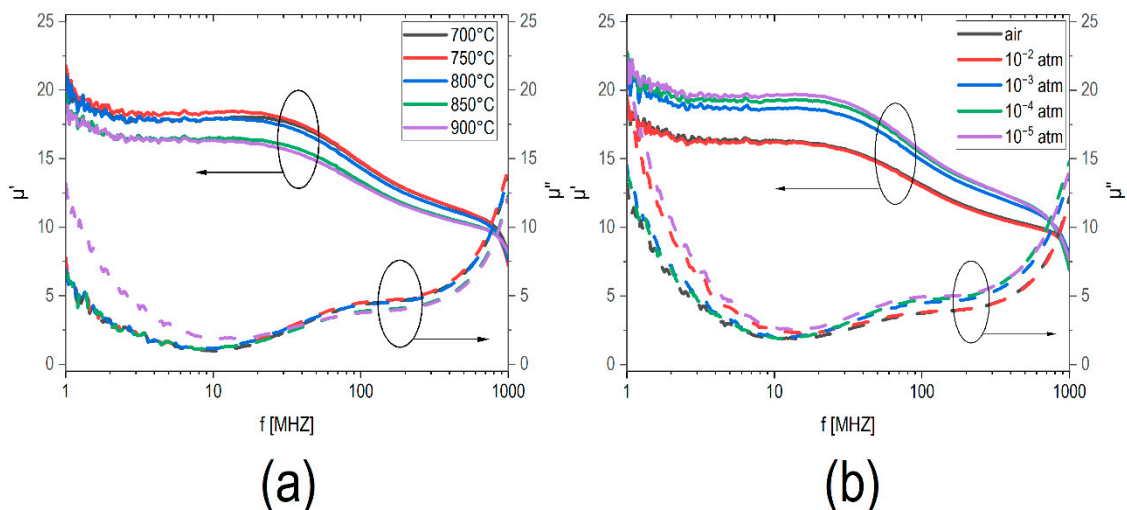


Figure 10. Permeability spectra of FeSiCr samples annealed at various temperatures in air (a) and at 900 °C under various oxygen partial pressures (b).

The permeability spectra showed slight variations in the permeability with frequency up to about 30 MHz, followed by a stronger decay in the hundreds of MHz region up to a resonance frequency at about 1 GHz (Figure 10). FeSiCr samples with higher permeability

of $\mu' = 44$ as presented in ref. [2] exhibited their resonance frequency at a lower frequency of about 100 MHz in agreement with Snoek's law.

The permeability at 1 MHz occurred at about $\mu' = 22$ for samples sintered in air at 700 °C and 750 °C and started to decrease from $\mu' = 21$ after annealing at 800 °C down to $\mu' = 18.5$ for samples annealed at 900 °C (Figure 9a). A similar behavior with a decrease in permeability after annealing at $T > 800$ °C was reported in ref. [4]. This reduction in permeability originates from the insulating Cr_2O_3 layer at the grain surfaces of the alloy particles. This layer seems to hinder domain wall motion and therefore lowers the permeability. Bulk chromium oxide Cr_2O_3 itself is an antiferromagnetic material. After nano-structuring into ultra-thin layers or as nanosized particles, it exhibits a weak ferromagnetism that increases with decreasing particle size [17,18]. However, it is expected that the (less magnetic) chromia surface layer weakens the exchange across particles and contributes to the permeability reduction. For samples annealed at 900 °C at different p_{O_2} values, the permeability increased from $\mu' = 18.5$ after annealing in air at 900 °C to about $\mu' = 22.5$ for samples annealed at $p_{\text{O}_2} = 10^{-5}$ atm (Figure 9b). Such increased permeability is consistent with the observations of less Cr_2O_3 formation under more reducing conditions.

FeSiCr alloys represent an interesting family of magnetic materials used for the fabrication of multilayer powder inductors. In this study, we compared the effect of the annealing temperature and oxygen partial pressure as parameters to tailor the oxidation state of the alloy particle surfaces and the corresponding performance of the material. It has been known that increasing annealing temperatures enhance the formation of a Cr_2O_3 oxide surface layer and, hence, the resistivity of the alloy, but also reduce permeability. It has been documented here that a reduction of the oxygen partial pressure during annealing at 900 °C is an option to reduce and slow down the formation of a chromia layer of sufficient thickness and, simultaneously, avoid the reduction of permeability upon annealing at 900 °C. This offers new paths for firing multilayer inductors with enhanced performance including high insulation resistance and permeability, or inductance.

4. Conclusions

FeSiCr alloy is an important soft magnetic material for multilayer power inductors. Upon processing of the multilayer, the alloy is laminated at high pressure and annealed in air. During annealing, a surface layer of Cr_2O_3 forms, which markedly affects the electromagnetic performance. We have studied the effect of annealing temperature in air and, alternatively, the effect of oxygen partial pressure during annealing at 900 °C on the formation of the surface oxide layer and the performance.

With increasing annealing temperature in air:

- The alloy oxidation and chromia layer formation increased.
- The alloy composition became more Fe-rich.
- The insulation resistance increased and the permeability decreased.

With decreasing oxygen partial pressure in the gas atmosphere during annealing at 900 °C:

- The formation of an insulating Cr_2O_3 surface layer slowed down.
- The resistivity decreased somewhat and the permeability increased.

This implies that the p_{O_2} of the gas atmosphere is another important parameter that allows for tailoring the insulating layer thickness and hence the insulating resistance, as well as the electromagnetic performance of FeSiCr-based inductors. These findings will be used to derive optimum annealing regimes of FeSiCr/ferrite composite multilayer inductors with sufficient insulation resistance of the FeSiCr, with negligible Ag migration in the magnetic layers and/or less reaction between Ag and magnetic materials.

Author Contributions: Conceptualization, J.T.; methodology, C.P. and J.T.; validation, C.P.; investigation, C.P.; data curation, C.P. and J.T.; writing—original draft preparation, C.P. and J.T.; writing—review and editing, J.T.; supervision, J.T.; project administration, J.T.; funding acquisition, J.T. All authors have read and agreed to the published version of the manuscript.

Funding: This work was funded by the Deutsche Forschungsgemeinschaft DFG (Germany) with grant No. 165/9-1.

Data Availability Statement: Not applicable.

Acknowledgments: The authors acknowledge H.I. Hsiang (Cheng Kung Univ. Tainan, Taiwan) for providing the FeSiCr powder and for inspiring discussions.

Conflicts of Interest: The authors declare no conflict of interest.

References

1. Shokrollahi, H.; Janghorban, K. Soft magnetic composite materials (SMCs). *J. Mater. Proc. Techn.* **2007**, *189*, 1–12. [[CrossRef](#)]
2. Shiroki, K.; Kawano, K.; Matsuura, H.; Kishi, H. New type composite material for SMD power inductor. *J. Jpn. Soc. Powder Metall.* **2014**, *61* (Suppl. S1), S242–S244. [[CrossRef](#)]
3. Hsiang, H.I. Progress in materials and processes of multilayer power inductors. *J. Mater. Sci: Mater. Electr.* **2020**, *31*, 16089–16110. [[CrossRef](#)]
4. Hsiang, H.I.; Fan, L.F.; Ho, K.T. Relationship between the microstructure and magnetic properties of Fe-Si-Cr powder cores. *IEEE Trans. Magn.* **2018**, *54*, 1–7. [[CrossRef](#)]
5. Chen, Z.; Liu, X.; Kan, X.; Wang, Z.; Zhu, R.; Yang, W.; Wu, Q.; Shezad, M. Phosphate coatings evolution study and effects of ultrasonic on soft magnetic properties of FeSiAl by aqueous phosphoric acid solution passivation. *J. Alloys Compd.* **2019**, *783*, 434–440. [[CrossRef](#)]
6. Zhou, B.; Dong, Y.; Chi, Q.; Zhang, Y.; Chang, L.; Gong, M.; Huang, J.; Pan, Y.; Wang, X. Fe-based amorphous soft magnetic composites with SiO₂ insulation coatings: A study on coatings thickness, microstructure and magnetic properties. *Ceram. Int.* **2020**, *46*, 13449–13459. [[CrossRef](#)]
7. Wu, S.; Dong, Y.; Li, X.; Gong, M.; Zhao, R.; Gao, W. Microstructure and magnetic properties of FeSiCr soft magnetic powder cores with MgO insulating layer prepared by the sol-gel method. *Ceram. Intl.* **2022**, *48*, 22237–22245. [[CrossRef](#)]
8. Yaghtin, M.; Taghvaei, A.H.; Hashemi, B.; Langhorban, K. Effect of heat treatment on magnetic properties of iron-based soft magnetic composites with Al₂O₃ insulation coating produced by sol-gel method. *J. Alloys Compd.* **2013**, *581*, 293–297. [[CrossRef](#)]
9. Zhao, X.; Lv, Q.; Kann, X.; Liu, X.; Feng, S. Improved magnetic properties of FeSiCr soft magnetic composites by adding strontium ferrite. *J. Electr. Mater.* **2022**, *51*, 6777–6783. [[CrossRef](#)]
10. Wu, Y.P.; Chiang, H.Y.; Hsiang, H.I. Interaction between silver inner electrode and Fe-Si-Cr alloy of metal multilayer chip inductors. *AIP Adv. Phys.* **2018**, *8*, 085006. [[CrossRef](#)]
11. Wu, Y.P.; Hsiang, H.I. Sintering temperature and atmosphere effects on electric and magnetic properties of multilayer FeSiCr alloy inductors. *Mat. Sci. Engin. B* **2022**, *275*, 115523. [[CrossRef](#)]
12. Hsiang, H.I.; Yang, S.M.; Chen, C.C. Effects of CuO content in the glass on the interfacial reaction for the NiCuZn ferrites-FeSiCr alloy composite. *Intl. J. Appl. Glass Sci.* **2020**, *11*, 774–783. [[CrossRef](#)]
13. Davey, W.P. Lattice constants of twelve common metals. *Phys. Rev.* **1925**, *25*, 753–761. [[CrossRef](#)]
14. Newnham, R.E.; de Haan, Y.M. Refinement of the alpha Al₂O₃, Ti₂O₃, V₂O₃, Cr₂O₃ structures. *Z. Krist.* **1962**, *117*, 235–237. [[CrossRef](#)]
15. Abrahamson, E.P.; Lopata, S.L. The lattice parameters and solubility limits of alpha iron as affected by some binary transition element additions. *Trans. Metall. Soc. AIME* **1966**, *236*, 76–87.
16. Sutton, A.; Hume-Rothery, W. The lattice spacings of solid solutions of titanium, vanadium, chromium, manganese, cobalt and nickel in α -iron. *Philos. Mag.* **1955**, *46*, 1295–1309. [[CrossRef](#)]
17. Vollath, D.; Szabo, D.V.; Willis, J.O. Magnetic properties of nanocrystalline Cr₂O₃ synthesized in a microwave plasma. *Mater. Lett.* **1996**, *29*, 271–279. [[CrossRef](#)]
18. Balachandran, U.; Siegel, R.W.; Liao, Y.X.; Askew, T.R. Synthesis, sintering and magnetic properties of nanophase Cr₂O₃. *Nanostructured Mater.* **1995**, *5*, 505–512. [[CrossRef](#)]